

Supporting Information

In Situ Raman Spectroscopy of Copper and Copper Oxide Surfaces during Electrochemical Oxygen Evolution Reaction: Identification of Cu^{III} Oxides as Catalytically Active Species

Yilin Deng,[†] Albertus D. Handoko,[†] Yonghua Du,[‡] Shibo Xi,[‡] and

Boon Siang Yeo^{*,†,§}

[†]Department of Chemistry, Faculty of Science, National University of Singapore, 3 Science Drive 3,
Singapore 117543

[‡]Institute of Chemical and Engineering Sciences, A*STAR, 1 Pesek Road, Jurong Island,
Singapore 627833

[§]Solar Energy Research Institute of Singapore, National University of Singapore, 7 Engineering
Drive 1, Singapore 117574

*Author to whom correspondence should be addressed to: chmyeos@nus.edu.sg, Fax: +65 6779
1691, Tel: +65 6516 2836

S1. Electrochemical/Raman setup

The schematic diagram of the electrochemical/Raman spectroscopy system is shown in Figure S1.

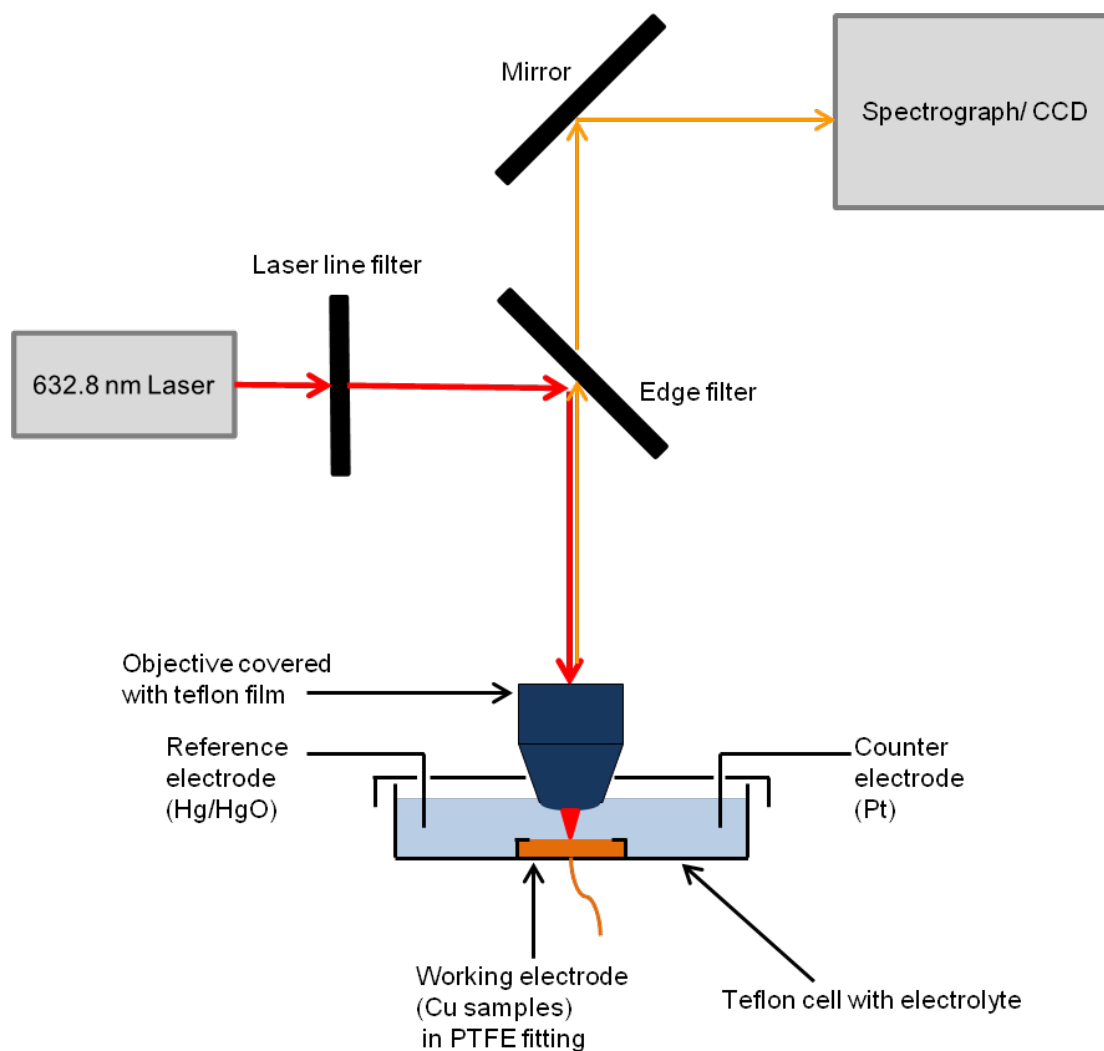


Figure S1: Schematic diagram of the electrochemical/Raman spectroscopy setup.

S2. Electrochemical/X-ray absorption spectroscopy (XAS) setup

The schematic diagram of the electrochemistry/XAS setup is shown in Figure S2.

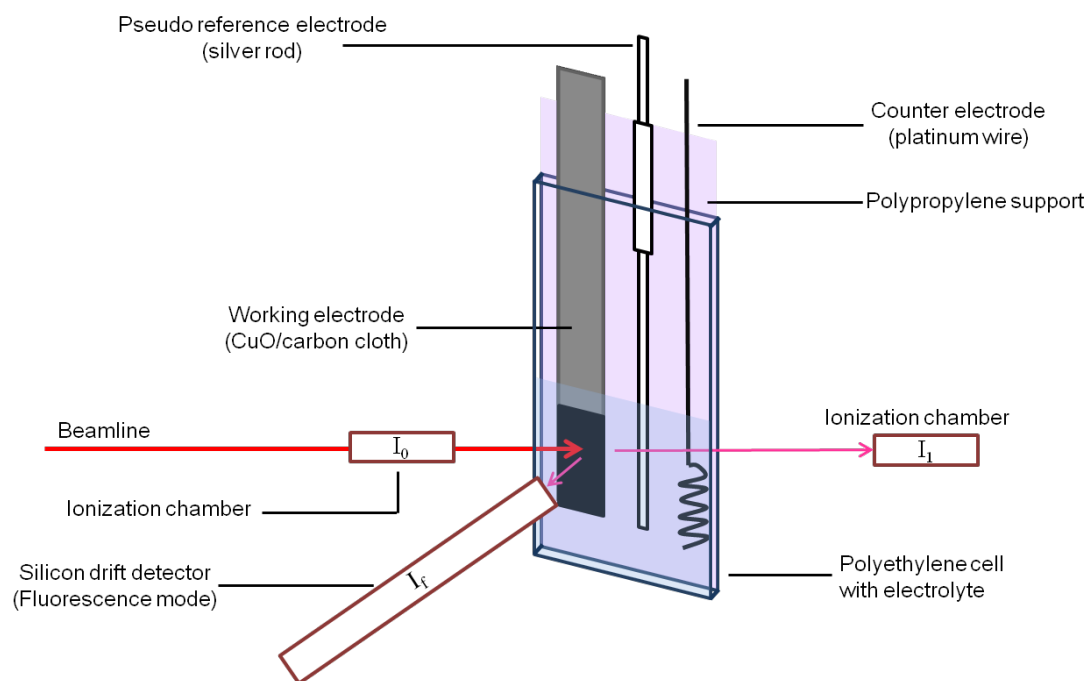


Figure S2: Schematic diagram of electrochemical/XAS setup.

S3. Electrochemical measurements of the four Cu electrodes in the dark

Cyclic voltammetry and chronoamperometry of the Cu electrodes were performed in the dark (Figures S3 and S4). The electrochemical data obtained were similar to those shown in Figures 3a and 4a (collected during *in situ* Raman spectroscopy). This demonstrates that illumination from the laser did not affect the electrochemical measurements.

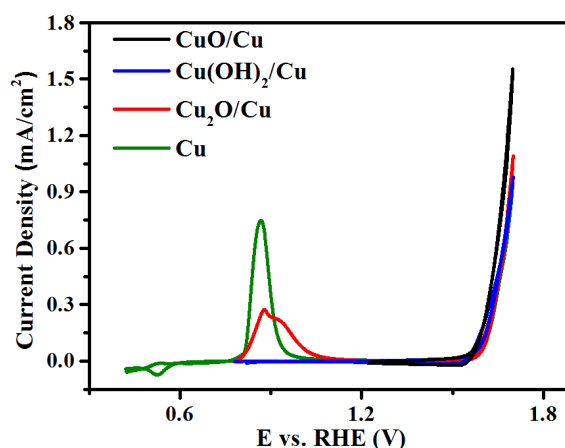


Figure S3: Cyclic voltammograms of the Cu, $\text{Cu}_2\text{O}/\text{Cu}$, $\text{Cu}(\text{OH})_2/\text{Cu}$ and CuO/Cu samples in 0.1 M KOH electrolyte without laser illumination. Scan rate: 1 mV/s.

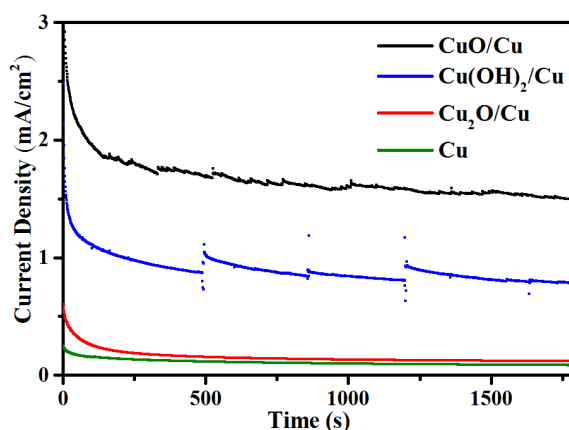


Figure S4: Chronoamperograms of Cu, $\text{Cu}_2\text{O}/\text{Cu}$, $\text{Cu}(\text{OH})_2/\text{Cu}$ and CuO/Cu samples at 1.7 V in 0.1 M KOH electrolyte without laser illumination.

S4. Characterization of Cu samples by atomic force microscopy

AFM images and their analysis for Cu, Cu₂O/Cu, Cu(OH)₂/Cu and CuO/Cu samples after OER are shown in Figures S5 and S6, and Tables S1 and S2. These images were used for estimating the surface areas of the Cu catalysts as the latter underwent morphological changes to various degrees during OER. Thus, it would be fairer to normalize the resultant electrochemical currents using surface areas estimated from post-OER samples. The appearances of the AFM and SEM images are consistent with each other. For example, the SEM (Figure 4c(i)) and AFM (Figure S6a) images of a Cu surface after chronoamperometry at 1.7 V are similar. We are aware that AFM does not measure any porosity that could be present in the Cu catalysts. However, there is no evidence to suggest that these materials are porous. We also note that there is no ‘perfect’ method to measure the true surface areas of catalysts. However, by consistently using AFM as the measurement method, we could ensure a self-consistent estimation of the surface areas on all Cu electrodes. The roughness factors of electrodeposited films determined from AFM have also been demonstrated by Gira et al. to correlate well to the roughness factors obtained from the double-layer capacitance method.¹

S4.1. AFM images and analysis of the four Cu samples after cyclic voltammetry and chronoamperometry

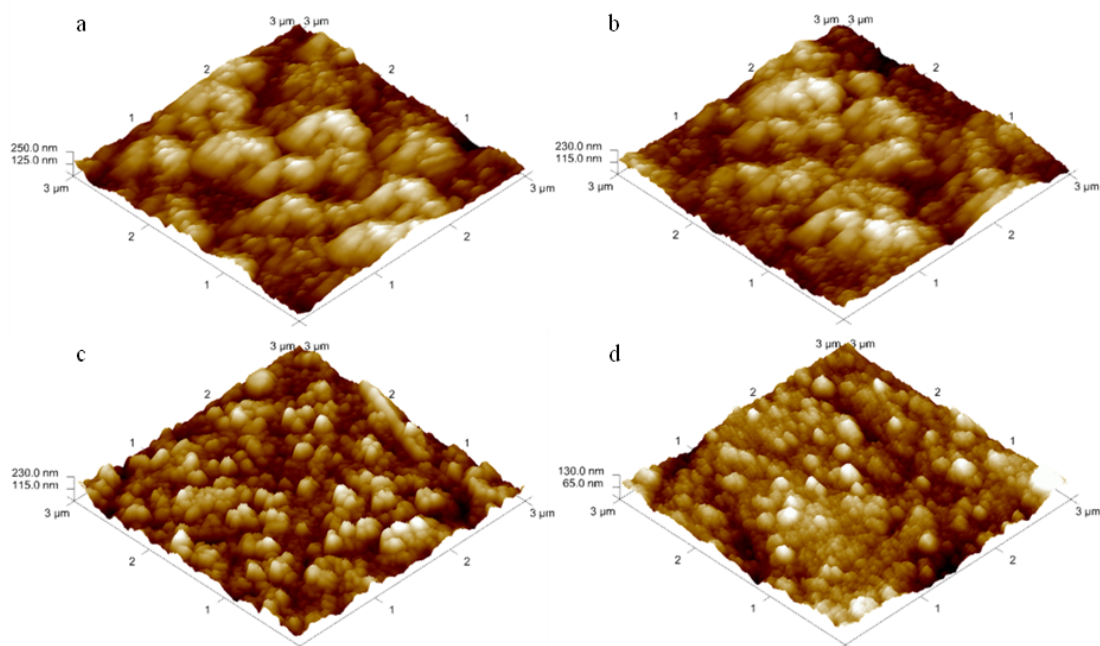


Figure S5: Atomic force microscopy images of (a) Cu, (b) Cu₂O/Cu, (c) Cu(OH)₂/Cu and (d) CuO/Cu samples, after they were subjected to cyclic voltammetry and 1800 s of chronoamperometry at 1.7 V in 0.1 M KOH solution.

Table S1 Analysis of atomic force microscopy (AFM) results

Sample	Geometric surface area / μm^2	AFM-determined surface area/ μm^2	Surface area difference
Cu	9.00	10.6	18.0 %
Cu ₂ O/Cu	9.00	10.6	18.0 %
Cu(OH) ₂ /Cu	9.00	12.9	43.5 %
CuO/Cu	9.00	9.99	11.0 %

S4.2. AFM analysis of the four Cu samples after direct chronoamperometry at 1.7 V

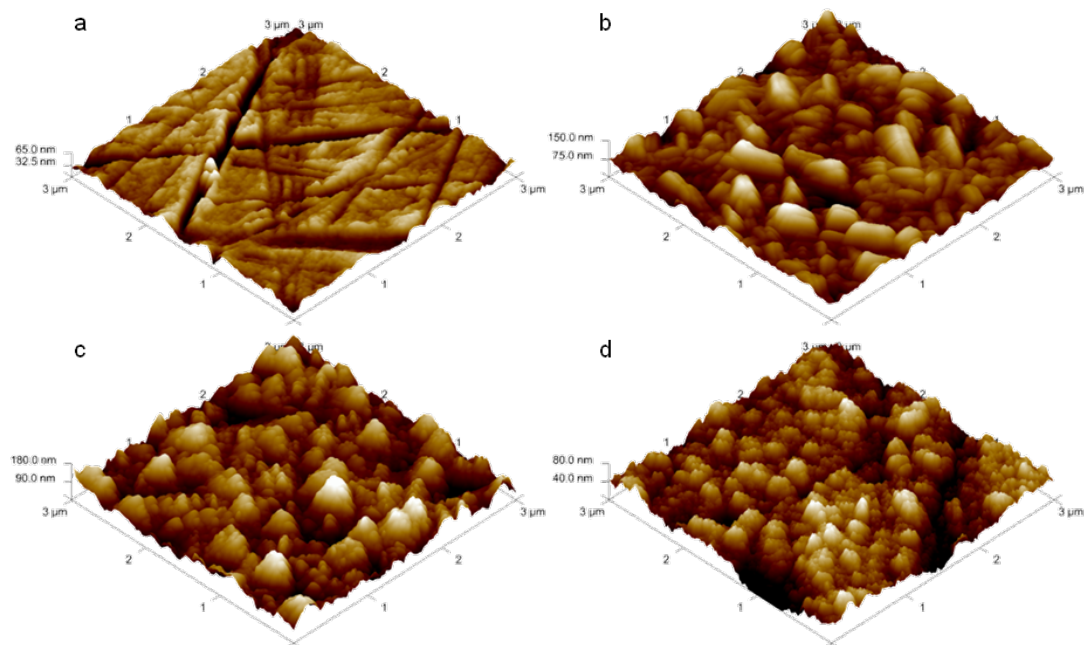


Figure S6: Atomic force microscopy images of (a) Cu, (b) $\text{Cu}_2\text{O}/\text{Cu}$, (c) $\text{Cu}(\text{OH})_2/\text{Cu}$ and (d) CuO/Cu samples after 1800 s chronoamperometry measurements at 1.7 V.

Table S2 Analysis of atomic force microscopy (AFM) results

Sample	Geometric surface area/ μm^2	AFM-determined surface area/ μm^2	Surface area difference
Cu	9.00	9.29	3.24 %
$\text{Cu}_2\text{O}/\text{Cu}$	9.00	9.55	6.10 %
$\text{Cu}(\text{OH})_2/\text{Cu}$	9.00	10.6	18.0 %
CuO/Cu	9.00	9.53	5.86 %

S5. Tafel plots of Cu samples at OER-relevant potentials

S5.1. Cyclic voltammograms and Tafel plots of the four Cu electrodes

Cyclic voltammetry measurements which scan through the active regions of Cu (~ 0.45 - 1.10 V) would oxidize the surfaces of the Cu and $\text{Cu}_2\text{O}/\text{Cu}$ samples to CuO and $\text{Cu}(\text{OH})_2$ (Figure S7a).² Hence, similar Tafel slope values of $60 - 66$ mV/dec were obtained from all the four samples (Figure S7b).

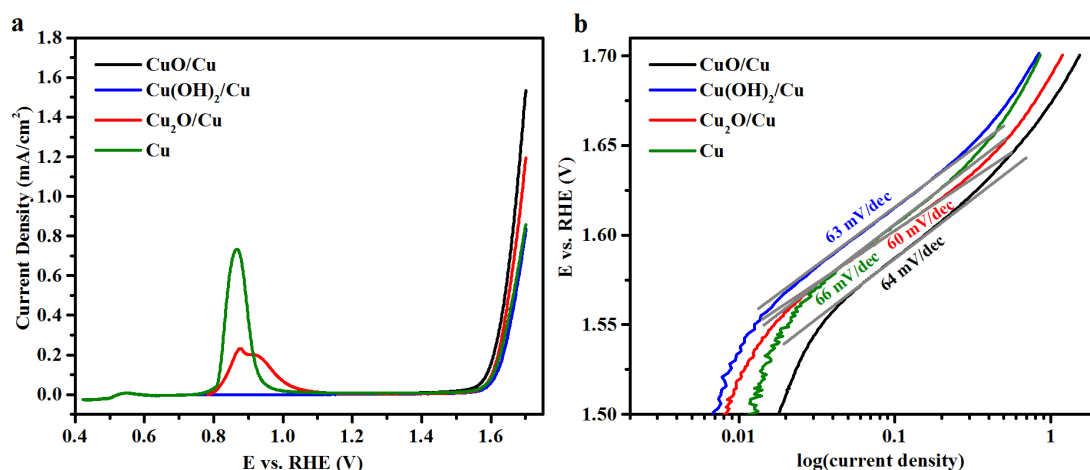


Figure S7: (a) Cyclic voltammograms and (b) corresponding Tafel plots of Cu, $\text{Cu}_2\text{O}/\text{Cu}$, $\text{Cu}(\text{OH})_2/\text{Cu}$ and CuO/Cu samples in 0.1 M KOH electrolyte. Only the anodic sweep of the CV is shown. Scan rate: 1 mV/s.

S5.2. Linear sweep voltammograms and Tafel plots of the four Cu electrodes (post-chronoamperometry)

Linear sweep voltammetry was performed on the four Cu samples after they have been subjected to only chronoamperometry at 1.7 V (Figure S8a). Significant oxidation of the Cu and Cu₂O/Cu samples could be minimized because the active regions of Cu at ~0.45-1.10 V were avoided.² The corresponding Tafel plots are shown in Figure S8b. Smaller Tafel slope values were obtained for CuO/Cu and Cu(OH)₂/Cu samples, in comparison with Cu₂O/Cu and Cu samples.

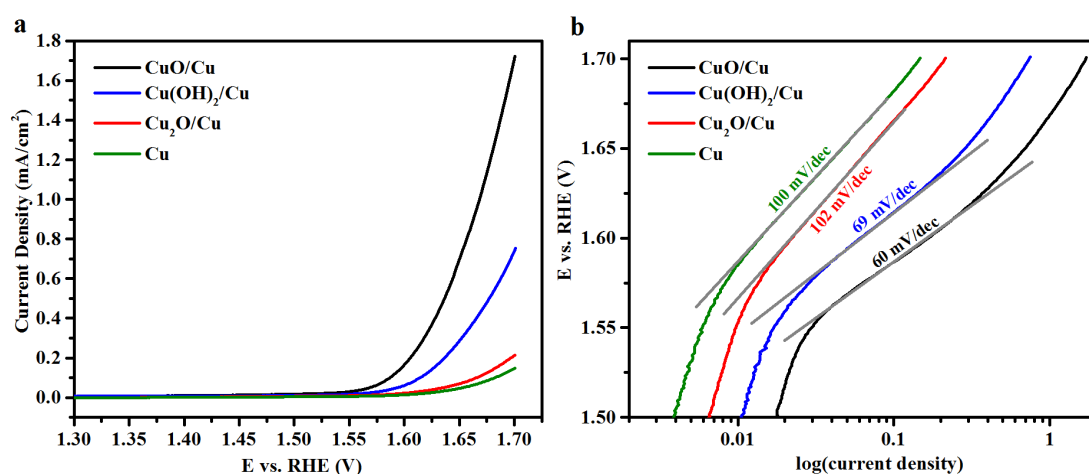


Figure S8: (a) Linear sweep voltammograms and (b) corresponding Tafel plots of Cu, Cu₂O/Cu, Cu(OH)₂/Cu and CuO/Cu electrodes (post-chronoamperometry) in 0.1 M KOH electrolyte. Scan rate: 1 mV/s.

S6. Estimation of the passivation reaction on Cu and Cu₂O/Cu electrodes during chronoamperometry at 1.7 V

S6.1. Cu electrode

After 1800 s chronoamperometry at 1.7 V was performed on the Cu electrode (Figure 4a), the electrolyte was purged with N₂ gas for 15 min to remove the O₂ gas. Linear sweep voltammetry (cathodic sweep) was then carried out on the same Cu sample at a scan rate of 10 mV/s (Figure S9). The featureless Raman spectrum of the electrode at -0.15 V (towards the end of the cathodic sweep) indicates that the sample had been reduced to Cu metal (Insert in Figure S9).

The charge beneath the cathodic peaks was estimated to be ~2.0 mC. This is an indication of the amount of oxides that could be formed during the chronoamperometry. The total charge measured during 1800 s chronoamperometry at 1.7 V was ~127.5 mC. Hence, the chronoamperometry current can be attributed to mainly (98 %) O₂ evolution rather than the passivation reaction of the Cu sample.

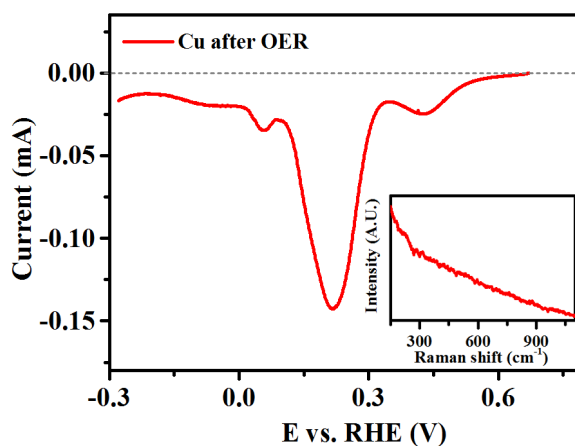


Figure S9: Linear sweep voltammogram (cathodic sweep) of a Cu sample after 1800 s chronoamperometry measurement at 1.7 V. Scan rate: 10 mV/s. The insert shows the Raman spectrum of the electrode collected at -0.15 V.

S6.2. Cu₂O/Cu electrode

To estimate the amount of oxides formed on a Cu₂O/Cu electrode during chronoamperometry at 1.7 V, linear sweep voltammetry (cathodic sweep) was first used to reduce the oxide on a freshly-prepared Cu₂O/Cu sample (Figure S10). Linear sweep voltammetry was also performed on a second Cu₂O/Cu sample, but only after it was subjected to 1800 s chronoamperometry at 1.7 V. The featureless Raman spectrum of the electrode at -0.4 V (towards the end of the cathodic sweep) indicates that all oxide had been reduced to Cu metal (Figure S10, insert).

The charges beneath the reduction peaks of these two linear sweep voltammograms were respectively 108.7 mC (freshly-prepared Cu₂O/Cu) and 110.0 mC (Cu₂O/Cu after chronoamperometry). Hence, 1.3 mC of charge could be assigned to the formation of amorphous Cu oxides during chronoamperometry. The total charge measured during the chronoamperometry at 1.7 V was ~147.6 mC. This implies that the current observed during the chronoamperometry can be attributed to mainly (99 %) O₂ evolution rather than further oxidation reaction of the Cu₂O/Cu sample.

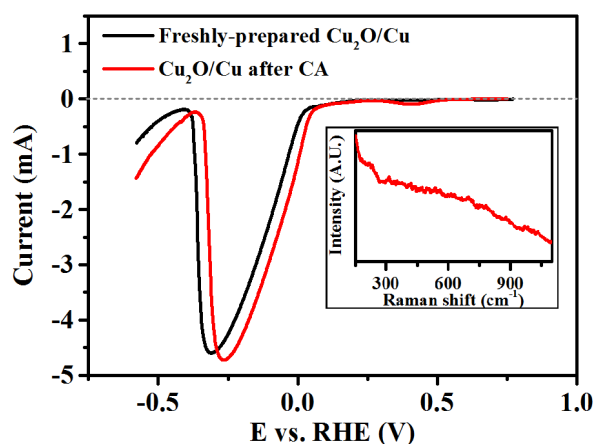


Figure S10: Linear sweep voltammograms (cathodic sweep) of a freshly-prepared Cu₂O/Cu sample (black curve) and a Cu₂O/Cu sample after 1800 s chronoamperometry measurement at 1.7 V (red curve). Scan rate: 10 mV/s. The insert shows the Raman spectrum of the electrode at -0.4 V.

S7. Comparison between the Raman spectra collected on a CuO/Cu sample during OER and NaCuO₂ standard

The Raman spectrum of freshly-prepared NaCuO₂ powder was measured, and compared against that of a CuO/Cu electrode at 1.7 V in 0.1 M KOH (Figure S11).^{3,4} Each presented spectrum is an average of three continuously-acquired spectra of collection time 10 s each.

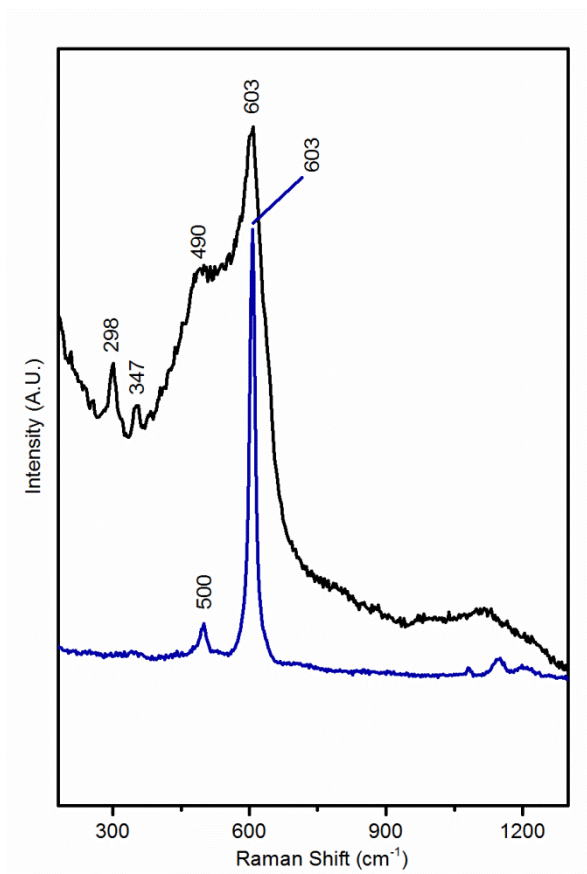


Figure S11: Raman spectra of CuO/Cu sample at 1.7 V in 0.1 M KOH (black curve) and NaCuO₂ standard (blue curve).

S8. Oxygen evolution in 0.1 M KOH and 0.1 M KOD electrolyte

In situ Raman spectroscopy was performed on CuO/Cu at 1.7 V in both 0.1 M KOH and 0.1 M KOD electrolytes (98 atom % D, 40 wt. % KOD in D₂O solution, Sigma Aldrich; 99.9 atom % D, D₂O, Cambridge Isotope Laboratories). The 603 cm⁻¹ peak did not exhibit any frequency shift when the KOH electrolyte was replaced with KOD electrolyte (Figure S12). This shows that the 603 cm⁻¹ vibration did not involve chemical bonds containing H.

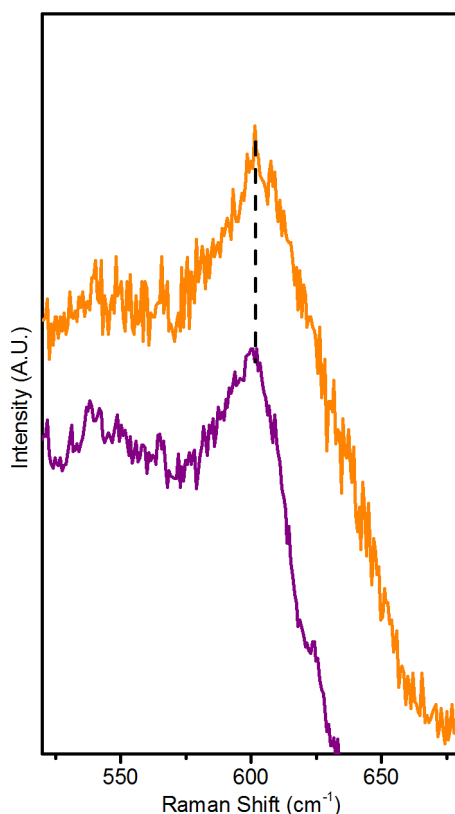


Figure S12: Raman spectra collected at 1.7 V on CuO/Cu sample in 0.1 M KOH (purple curve) and 0.1 M KOD electrolyte (orange curve).

S9. In-situ XANES on CuO/carbon cloth at O₂-evolving potentials

S9.1 The Cu K-edge XANES of CuO/carbon cloth (2.0 V, in 0.1 M KOH), CuO and NaCuO₂ standards

The Cu K-edge XANES spectra of a CuO/carbon cloth sample poised at 2.0 V in 0.1 M KOH electrolyte, as well as NaCu^{III}O₂ and Cu^{II}O standards are presented in Figure S13a. The first and second derivatives of their normalized spectra are shown in Figures S13b and c.

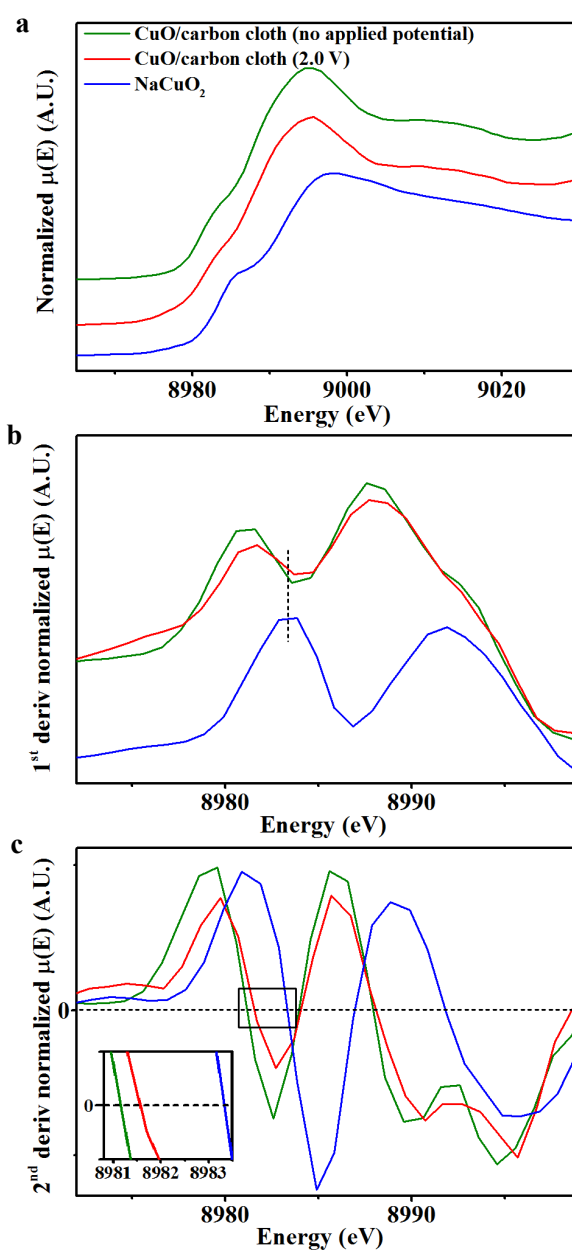


Figure S13: (a) The Cu K-edge XANES spectra of CuO/carbon cloth held at 2.0 V, with CuO and NaCuO₂ standards. (b) First and (c) second derivative of the XANES spectra shown in (a).

S9.2. Estimation of Cu^{III} population on the CuO/carbon cloth sample at OER-evolving potentials

The cyclic voltammogram of CuO/carbon cloth was measured (cathodic sweep first, Figure S14). A cathodic peak at ~ 1.55 V, which can be attributed to the reduction of Cu^{III} to Cu^{II} , was observed.^{5,6} Another reduction peak at ~ 0.05 V corresponds to the reduction of bulk CuO metal.⁷ Based on the amount of charges beneath these two reduction peaks (3.3 mC and 94 mC respectively), the amount of Cu^{III} present in the sample at OER potentials was estimated to be $\sim 7\%$.

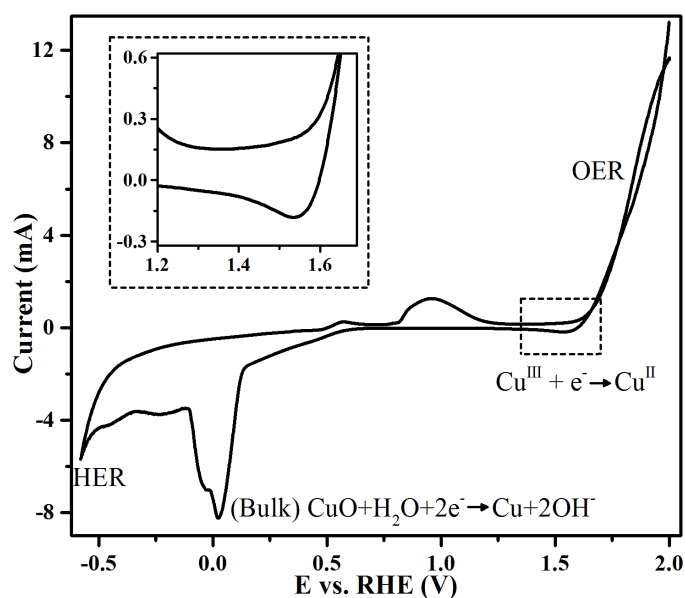


Figure S14: The cyclic voltammogram of CuO/carbon cloth (cathodic sweep first) in 0.1 M KOH electrolyte. Scan rate: 10 mV/s.

S10. Reaction of NaCuO₂ with 0.1 M KOH solution

Freshly prepared NaCuO₂ was added to aqueous 0.1 M KOH solution. The former quickly decomposed to give a black powder and O₂ gas. XRD and Raman spectroscopy of the black powder indicate that it is CuO (Figure S15).³ Furthermore, elemental analysis of the KOH solution by ICP-OES showed a negligible concentration of Cu (0.66 ppm) compared to Na (8342 ppm). This shows that the Cu ions formed from the decomposition of NaCuO₂ in KOH is likely to stay as insoluble CuO_(s), rather than soluble Cu ions.

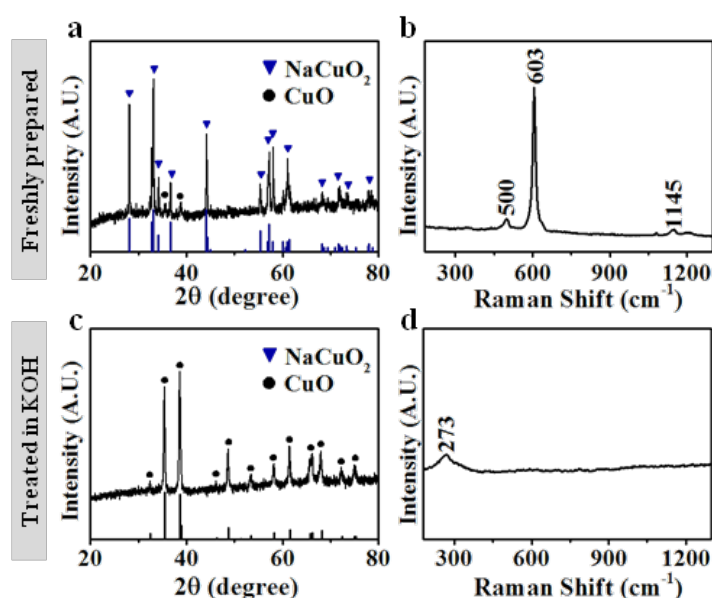


Figure S15: (a) X-ray diffractogram and (b) Raman spectrum of freshly-prepared NaCuO₂. (c) X-ray diffractogram and (d) Raman spectrum of the NaCuO₂ powder after it was treated in 0.1 M KOH solution.

References

- (1) Gira, M. J.; Tkacz, K. P.; Hampton, J. R. *Nano Convergence* **2016**, 3: 6.
- (2) Landolt, D. In *Corrosion and Surface Chemistry of Metals*; 1st ed.; EFPL Press: Lausanne, Switzerland, 2007, p 227-274.
- (3) Popova, T. V.; Aksenova, N. V. *Russ. J. Coord. Chem.* **2003**, 29, 743-765.
- (4) Ruther, R. E.; Zhou, H.; Dhital, C.; Saravanan, K.; Kercher, A. K.; Chen, G.; Huq, A.; Delnick, F. M.; Nanda, J. *Chem. Mater.* **2015**, 27, 6746-6754.
- (5) Miller, B. *J. Electrochem. Soc.* **1969**, 116, 1675-1680.
- (6) Abd el Haleem, S. M.; Ateya, B. G. *J. Electroanal. Chem. Interfacial Electrochem.* **1981**, 117, 309-319.
- (7) Nakayama, S.; Kaji, T.; Shibata, M.; Notoya, T.; Osakai, T. *J. Electrochem. Soc.* **2007**, 154, C1-C6.